

Rapid ungated myocardial perfusion MRI with an undersampled radial CAIPI acquisition and a compressed sensing reconstruction

Ganesh Adluru¹, Liyong Chen², Eugene Kholmovski¹, John Roberts¹, and Edward V.R. DiBella¹

¹Radiology, University of Utah, Salt Lake City, Utah, United States, ²Advanced MRI Technologies, CA, United States

Introduction: Myocardial perfusion imaging is a distinctive tool for determining the downstream effects of narrowed/blocked coronary arteries on the myocardium. High in-plane spatial resolution and increased slice coverage are desired without sacrificing the rapid temporal dynamics of injected contrast agent. Undersampled k-space acquisitions combined with advanced reconstruction methods like compressed sensing [1-4] overcome the limitations of conventional imaging and result in increased slice coverage without sacrificing spatial and temporal resolutions. These frameworks also facilitated fast ungated imaging; a simpler promising method compared to standard ECG gated myocardial perfusion MRI [5-9]. A complementary slice acceleration approach termed CAIPIRINHA [10] (abbreviated here as CAIPI) was recently applied for gated perfusion acquisitions along with Cartesian k-space undersampling [11]. Slice GRAPPA reconstruction to separate the simultaneously acquired slices was followed by a separate CS reconstruction step to remove ghosting artifacts from k-space undersampling [11]. Here we implement a simultaneous multi-slice radial CAIPI acquisition from [12] with k-space undersampling and a joint compressed sensing reconstruction [13] for increased slice coverage without sacrificing spatial and temporal resolutions. Promising results with the proposed framework are presented for ungated perfusion acquisitions.

Methods: Ungated radial CAIPI data with a slice acceleration factor (CAIPI factor) of two was acquired on a Siemens 3T Verio scanner using a 32 channel cardiac coil. Ignoring the ECG gating, after each saturation pulse and a saturation recovery time of 30 msec, four CAIPI slices were consecutively acquired to give a total of eight short-axis slices from apex to base. Golden ratio based angle spacing [14] was used between the rays in-plane and an alternating phase modulation of 0, π was applied for every ray of the second slice of the excited pair. Acquisition matrix (readout x number of rays) was 144 x 24, TR=2.8 msec, TE=1.5 msec, field of view=250 mm², flip angle=12°, slice thickness=8mm with a spacing of 1.6 mm between adjacent slices, Gd dose=0.06mmol/kg. Reconstruction of a slice pair from each of the four CAIPI slices was performed in an iterative compressed sensing framework by minimizing the cost functional \mathcal{C} in (1).

$$\mathcal{C} = \sum_{i=1}^{nc} \left\| \left(\sum_{j=1}^{nsl} \emptyset_j (GS_{ij} I_j) \right) - d_i \right\|_2^2 + \alpha_t \sum_{j=1}^{nsl} TV_t(I_j) + \alpha_s \sum_{j=1}^{nsl} TV_s(I_j) \quad (1)$$

In (1) d_i is the acquired radial CAIPI data for coil i , nc (= 32 here) is the number of receiver coils, I_j is image data corresponding to slice index j , nsl (= 2 here) is the number of simultaneously excited slices, S_{ij} is the coil-sensitivity for coil i and slice j , G is the gridding operator, performed using NUFFT [15], to map image data to radial k-space data and \emptyset_j phase modulates k-space data for slice j . The first term enforces data fidelity to the acquired CAIPI data. TV_t is the temporal total variation constraint [2] and TV_s is the 2D spatial total variation constraint [2]. α_t and α_s are weighting factors for temporal and spatial TV constraints respectively. Coil sensitivities for the eight slices were determined using a non-CAIPI radial acquisition performed after completion of Gd injection. A preliminary reconstruction using all of the acquired data for all time frames was first done as described above and images were binned into near systole and near diastole as described in [5,7]. k-space data corresponding to each bin was reconstructed separately using (1). This allows for more effective temporal TV regularization by reducing inter-frame motion effects on temporal sparsity in images.

Results: Figure 1 shows one time frame for eight slices at different cardiac phases from apex to base for a human (left) and a dog (right) dataset. The image quality is good overall with delineation of papillaries and small structures in the lung. Corresponding top and bottom slices shown with arrows and a yellow plus sign were simultaneously excited. All of the reconstructions converged within 40 iterations. To reconstruct a slice pair each with a matrix size of 288 x 288 and 50 time frames, on a standard CPU with parallel processing on 12 cores, each iteration took about a minute. Computation of TV constraints on the combined multi-coil image estimates from the 32 channel data took 0.6 secs each iteration while NUFFT operations consumed bulk of the time to perform gridding and inverse gridding operations.

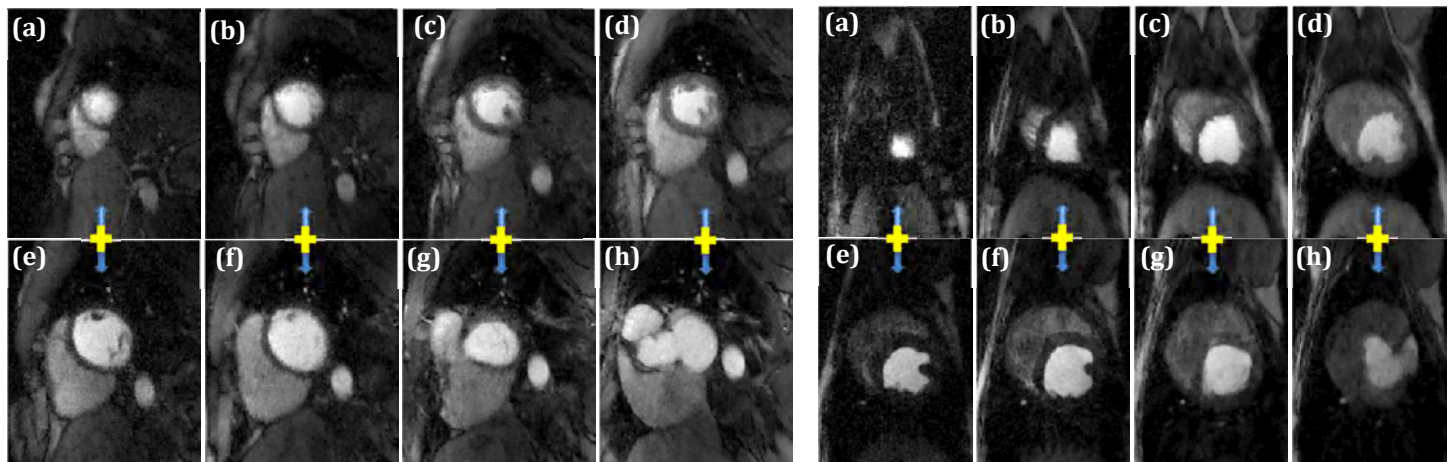


Figure 1: (a, h) One time frame for each of the eight slices from an ungated radial CAIPI acquisition and compressed sensing reconstruction. Corresponding top and bottom slices linked with arrows are simultaneously acquired. The left set of eight images is from a human study and the right set of images is from a dog study.

Discussion & Conclusion: Here we used the radial CAIPI framework to increase slice coverage and effectively acquire each slice in 37 msec repeating every 232 msec. Higher temporal resolution could be achieved by trading for fewer slices. Radial CAIPI acquisition with compressed sensing reconstruction is an exciting approach to increase coverage in ungated myocardial perfusion imaging without sacrificing temporal and spatial resolutions.

References: [1] Otazo et al MRM 64:767-76, 2010. [2] Adluru et al JMRI 29:466-72, 2009. [3] Pendersen et al MRM 62:706-16, 2009. [4] Lingala et al PMB 58:7309-27, 2013. [5] DiBella et al MRM 67:609-613, 2012. [6] Sharif et al MRM 2014 Epub [7] Harrison et al JCMR 15:26, 2013. [8] Chen et al MRM 2014 Epub. [9] Likhite et al To appear JCMR 2014. [10] Breuer et al MRM 53:684-91, 2005. [11] Stab et al JMRI 39:1575-87, 2014. [12] Yutzy et al MRM 65:1630-37, 2011. [13] Adluru et al #1532 ISMRM 2014. [14] Winkelmann et al. IEEE TMI 26:68-76, 2007. [15] Fessler et al IEEE TMI 51:560-574, 2003.